Attitude Sensor Alignment Calibration for the Solar Maximum Mission

Daniel S. Pitone

Computer Sciences Corporation

and

Malcolm D. Shuster

The Johns Hopkins University Applied Physics Laboratory

ABSTRACT

An earlier heuristic study of the fine attitude sensors for the Solar Maximum Mission (SMM) revealed a temperature dependence of the alignment about the yaw axis of the pair of fixed-head star trackers relative to the fine pointing Sun sensor. In the present work, new sensor alignment algorithms which better quantify the dependence of the alignments on the temperature are developed and applied to the SMM data. Comparison with the results from the previous study reveals the limitations of the heuristic approach. In addition, some of the basic assumptions made in the prelaunch analysis of the alignments of the SMM are examined. The results of this work have important consequences for future missions with stringent attitude requirements and where misalignment variations due to variations in the temperature will be significant.

1. INTRODUCTION

Because of the stringent attitude accuracy requirements, the temperature dependence of the alignments of the fine attitude sensors of the Solar Maximum Mission (SMM) has been closely studied.[1-5] These works have attempted to quantify the relationship between the variations in the SMM structural temperatures and the variations in the alignments of the fixed-head star trackers (FHSTs) relative to the fine pointing Sun sensors (FPSSs). The present work, which is an extension of Refs. 3 and 4, attempts to quantify more completely the relationship between the temperature and the alignments. This is done by using newly developed alignment estimation algorithms that can estimate the alignments better than the work in Refs. 3 and 4. In addition, the limiting assumptions made in the prelaunch analysis of the SMM with regard to the sensor alignments are examined.

One of the contributions of this work is a consistent framework for estimating the inflight alignments of spacecraft attitude sensors and investigating the nature of the changing alignments. An algorithm is provided for computing the alignments at a single temperature using inflight sensor measurements without the need to compute the spacecraft attitude and angular velocity. These alignment estimates at different temperatures are then input to a second algorithm which computes an optimal estimate for the temperature dependence. These methods can provide clues to the specific causes of the alignment changes and aid in the design of future structural configurations to minimize temperature effects.

This work begins by reviewing the heuristic analysis and its limitations as presented in Refs. 3 and 4. A brief outline of the new alignment algorithms is then given and simulations are provided to demonstrate their capabilities. Then the application of the algorithms to SMM data is presented and the dependence of the alignments on temperature is completely discussed. The last section discusses the assumptions made pertaining to the actual inflight SMM alignment estimation algorithms and possible modifications that would have made these algorithms more effective.

2. AN HEURISTIC EXAMINATION OF THE SMM ALIGNMENTS

SMM History and Configuration

The SMM was launched in February of 1980 from the Eastern Test Range into a low Earth orbit to study solar radiation at several wavelengths. In November of 1980 the reaction wheels that controlled the spacecraft failed. Thereafter, the spacecraft was put into a stabilizing spin mode to preserve the mission. During this time little scientific work was accomplished. In April of 1984 the mission was repaired in orbit by the Space Transportation System, after which it was returned to normal mission operation. The spacecraft functioned normally until December of 1989 when it reentered the Earth's atmosphere. Further details on the history of the SMM are given in Ref. 6.

The SMM was the first of the Multimission Modular Spacecraft (MMS) which were designed for repair and adaptation. It consisted basically of two separate components. The first component was the MMS component which consisted of the communications, power, and attitude control modules. The attitude control module included two FHSTs and a complete set of gyros which were used for fine attitude determination. The FHSTs were mounted together on a rigid structure inside the attitude control module to minimize alignment variations.

The second main component of the SMM was the payload component. It consisted of the SMM scientific payload and the SMM-specific attitude sensors. The scientific payload consisted of the instruments used to study the Sun. The SMM-specific attitude sensors were a redundant set of FPSSs and a set of coarse Sun sensors. The scientific instruments and the FPSSs were comounted on a rigid plate to minimize misalignment between them. The basic configuration of the SMM is shown in Fig. 1.

SMM Attitude Determination Configuration

The goal of the SMM attitude determination and control system was to point the boresights of the scientific instruments as accurately as possible, nominally to within 5 arc-sec, at specific locations on the Sun. To this end, the scientific instruments and the FPSSs were mounted on the same rigid instrument support plate with their boresights parallel. It was assumed that they would remain parallel and that the relative misalignments about all three axes would be null throughout the mission. Thus, the goal of the attitude determination system became to point the FPSSs at locations on the Sun to within 5 arc-sec (3σ).
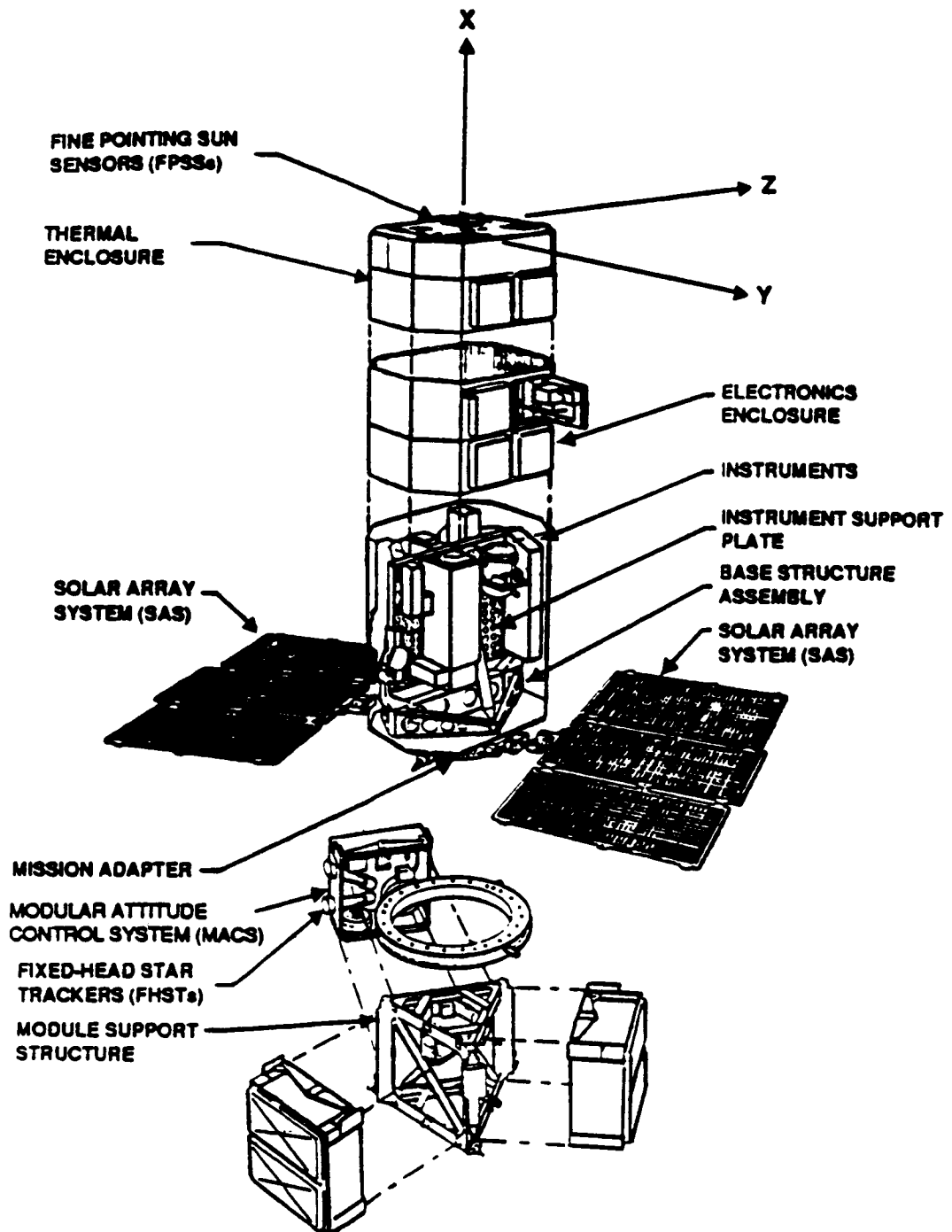
Figure 1. SMM Structure

The spacecraft attitude reference and body coordinate frames were defined so that the SMM attitude would be directly meaningful in terms of solar pointing. The reference frame was a noninertial frame in which the x-axis was defined to be the unit vector from the spacecraft to the Sun, the y-axis was defined as the unitized cross product of the x-axis and the direction of the solar north pole, and the z-axis completed the right-handed

orthogonal system. The body frame was defined by the FPSS coordinate axes. The x-axis of the body frame was defined as being parallel to the FPSS boresight. The y-, and z-axes of the body frame were defined as parallel to the z and negative y FPSS sensor axes. Thus, the output angles from the FPSS directly provided the attitude about the y- (pitch) and z-axes (yaw), which corresponded to the spherical coordinates of the pointing location on the Sun. Pointing the boresight of the FPSS (the x-axis of the spacecraft) to a specific location on the Sun required only successive pitch and yaw maneuvers.

The SMM FPSSs were vector sensors that measured rotations about two sensor axes and they had a field-of-view (FOV) of 2 deg × 2 deg and a specified accuracy of 5 arc-sec (3σ). Since the boresights of the two FPSSs were parallel, they provided attitude information only about two axes, corresponding to the pitch and yaw axes of the body reference system. The SMM FHSTs were also vector sensors that measured rotations about two sensor axes. These had an FOV of 8 deg × 8 deg and a specified accuracy of 30 arc-sec (3σ). The FOV's of the FHSTs did not overlap (i.e., their boresights were well separated). Thus, they could be used to compute a full three-axis attitude. Since the FPSSs provided only two axes of attitude information, the FHSTs were the prime source of roll attitude information.

The SMM Inflight Alignment Determination System

Since it was believed that the misalignment of the scientific instruments relative to the FPSSs would be negligible, the only alignment calibration needed was of the FHSTs relative to the FPSSs. Thus, a complete alignment calibration could be accomplished in orbit since the relative alignments are completely observable.[7] Therefore, for the SMM, the alignment calibration system should have been relatively simple and should have provided all the necessary alignment information necessary to compute the most accurate attitude of the spacecraft.

However, two assumptions were made in the prelaunch analysis of the alignments for the SMM that restricted the accuracy with which the alignments could be determined. The first assumption was, as stated above, that the alignment of the FPSSs relative to the scientific payload would not change. Since they were all mounted on a single rigid plate, it would seem that this was a valid assumption. However, because of it, no alignment calibration of the two FPSSs relative to each other was ever performed. If this assumption had not been made, the alignment of FPSS2 relative to FPSS1 could have been easily computed and the resulting value of the misalignment would have provided insight into the general level of misalignment between the FPSSs and the scientific payload.

The second assumption was that no roll alignment information of the two FHSTs relative to the FPSSs would be available. This followed supposedly from the fact that the FPSS boresights were parallel to the spacecraft body x-axis. Instead, it was assumed that the only roll alignment information available was the roll alignment of FHST2 relative to the roll alignment of FHST1. For this reason, the only alignment information ever calculated for the SMM were the pitch and yaw alignments of the FHSTs relative to FPSS1 and the roll alignment of FHST2 relative to FHST1.

The other notable point about the SMM alignment scheme was that the full inflight calibration algorithm generally required that the SMM be switched to an operating mode that eliminated the scientific data from the telemetry. The SMM scientists, however, were

very hesitant to switch to this mode except for absolutely necessary calibrations. When the alignment variation on the SMM was recognized, it was decided the alignment would be monitored each day. However, because the scientists could not be expected to agree to the mode switch every day, a pseudo-alignment algorithm that provided even less complete alignment information was devised in its place.

The pseudo-alignment algorithm was designed to monitor the pitch and yaw alignments of the FHSTs each day. It worked by subtracting the pitch and yaw attitude computed by the FHSTs from the pitch and yaw attitude computed by the FPSSs. The difference was attributed to misalignment of the FHSTs. Since the method worked by subtracting the computed attitudes, the alignments of the FHSTs were lumped together, i.e., it was assumed they moved as a single rigid element. Even though use of the pseudo-alignment algorithm provided very incomplete alignment information, it provided sufficiently good results that a characterization of the yaw alignment variation was possible. This will be further explored in the next section.

Review of Previous Work

Using the pseudo-alignment algorithm, it was discovered that the SMM FHSTs yaw alignment relative to FPSS1 varied over time and could be as large as 120 arc-sec. However, the pseudo-alignment algorithm showed no such variation for the alignments about the pitch axis. As mentioned earlier, it was thought that misalignment about the roll axis was unobservable.

An investigation into the possible causes of the alignment variation showed that the variation was correlated with the changing structural temperatures of the instrument support plate on which the FPSSs were mounted. After the data were filtered to remove some of the noise, a scatter plot could be constructed that showed the variation to be nearly linear. This scatter plot is shown in Fig 2. A least-squares straight line fit to the data yielded the following model for the yaw misalignment.

$$M = -130. \text{ arc-sec} + 11. \text{ T arc-sec}/^\circ\text{C} \quad , \qquad (2\text{-}1)$$

where M is the yaw misalignment and T is the spacecraft structural temperature which could be obtained from the regular telemetry. The computed accuracy of this equation, assuming the errors were normal and uncorrelated was 8.5 arc-sec (1σ).

Some questions still remained. For example, why was the yaw alignment temperature dependent while the pitch alignment seemingly was not? The previous work postulated an answer to this question which, however, was not demonstrated convincingly. In addition, because of the large amount of noise inherent in the pseudo-alignment calibration scheme, was it possible to better characterize the alignment dependence? In order to understand more fully the nature of the SMM alignments, it was decided to utilize more complete and rigorous methods of alignment determination to recalibrate the SMM alignments. This work is the subject of the remainder of this paper.
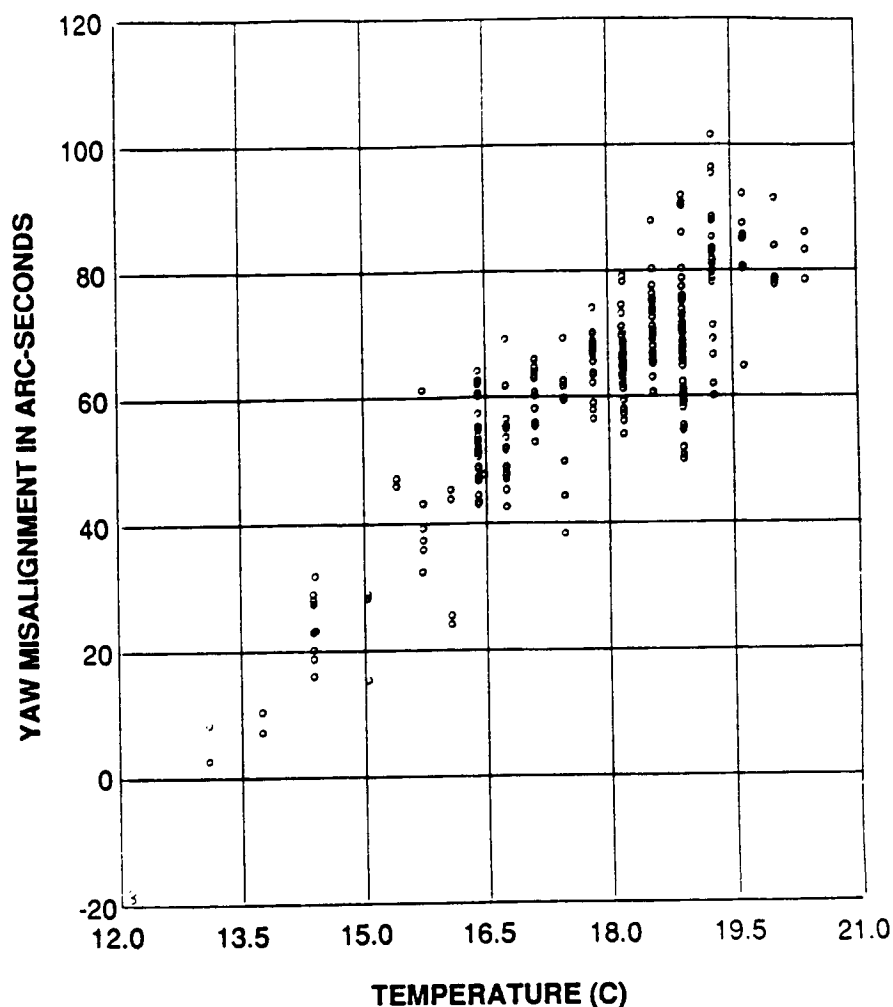
Figure 2. Scatter Plot of Yaw Misalignment and Temperature

3. A NEW BATCH ESTIMATOR OF SENSOR ALIGNMENTS

The batch alignment calibration algorithm used in this work[7-9] estimates alignments from derived attitude-independent effective measurements. (See also Ref. 10 for a comparison of this batch algorithm with sequential attitude-dependent algorithms.) This section reviews this algorithm and provides guidelines for its application. The reader is referred to Refs. 7 through 9 for a more complete description and derivation of the algorithm. A statistically correct method for computing the temperature dependence of the alignments will also be presented here. Realistic simulations are presented as well to demonstrate the power of these methods.

Basic Principles

The alignment matrix of a specific sensor i, denoted by S_i, may be defined as the orthogonal rotation matrix between the sensor coordinate frame and the body coordinate frame. This alignment matrix may be decomposed into two component rotation matrices. Thus, the alignment of sensor i at any time during the flight of a spacecraft may be written as

$$S_i = M_i S_i^o \quad , \tag{3-1}$$

where S_i^o is the prelaunch estimate of the sensor alignment matrix and M_i is the misalignment matrix, which represents the change in the alignment from the prelaunch value. The misalignment matrix may be represented by the rotation vector,[11] $\boldsymbol{\theta}_i$. If it is assumed that M_i represents a very small rotation, then

$$M_i = I + [[\boldsymbol{\theta}_i]] \quad , \tag{3-2}$$

where $[[\boldsymbol{\theta}_i]]$ is the antisymmetric matrix representation of a vector and can be defined as

$$[[\boldsymbol{\theta}_i]] = \begin{bmatrix} 0 & \theta_{i3} & -\theta_{i2} \\ -\theta_{i3} & 0 & \theta_{i1} \\ \theta_{i2} & -\theta_{i1} & 0 \end{bmatrix} \quad . \tag{3-3}$$

The vector, $\boldsymbol{\theta}_i$, which represents the misalignment of the sensor from its prelaunch value, is the quantity which is computed by the alignment algorithm.

To simplify the equations which follow, we define an uncalibrated observed vector as

$$\hat{\mathbf{W}}_{i,k}^o \equiv S_i^o \hat{\mathbf{U}}_{i,k} \quad , \tag{3-4}$$

where $\hat{\mathbf{U}}_{i,k}$ is the observed vector by sensor i, $i = 1, 2, \ldots, n$, at time t_k, $k = 1, 2, \ldots, N$, in the sensor coordinate frame. Thus, $\hat{\mathbf{W}}_{i,k}^o$ is the representation of the observed vector in the body frame uncorrected for the misalignment of the sensor from the prelaunch alignment estimate.

The effective attitude-independent scalar measurement used in this work is the difference of the cosine of the angle between the observed vectors of sensors i and j from the cosine of the angle between the corresponding reference vectors. Assuming that the misalignments and the sensor noise is small, the effective measurement equation can be derived as

$$z_{ij,k} = \hat{\mathbf{W}}_{i,k}^o \cdot \hat{\mathbf{W}}_{j,k}^o - \hat{\mathbf{V}}_{i,k} \cdot \hat{\mathbf{V}}_{j,k} = (\hat{\mathbf{W}}_{i,k}^o \times \hat{\mathbf{W}}_{j,k}^o) \cdot (\boldsymbol{\theta}_i - \boldsymbol{\theta}_j) + \Delta z_{ij,k} \quad , \tag{3-5}$$

where $\Delta z_{ij,k}$, the effective measurement noise, is

$$\Delta z_{ij,k} = \hat{\mathbf{W}}_{i,k}^o \cdot \Delta\hat{\mathbf{W}}_{j,k}^o + \hat{\mathbf{W}}_{j,k}^o \cdot \Delta\hat{\mathbf{W}}_{i,k}^o \quad , \tag{3-6}$$

where we have assumed that the errors in the observations are much larger than those in the reference vectors.

For the system of n attitude sensors, these scalar measurements at a common time t_k may be collected in a single column vector which we may write as

$$\mathbf{Z}_k = H_k \boldsymbol{\Theta} + \Delta \mathbf{Z}_k \quad , \tag{3-7}$$

where H_k and $\Delta \mathbf{Z}_k$ are determined from equations (3-5) and (3-6). Since at any time t_k, n sensed unit vectors correspond to $2n$ equivalent one-dimensional measurements, and three measurements are needed to determine the attitude, there can be only $2n - 3$ independent $z_{ij,k}$ at t_k. Thus, if we wish the covariance matrix of $\Delta \mathbf{Z}_k$ to be full-rank, then $\mathbf{Z}_k$ and $\Delta \mathbf{Z}_k$ are $(2n - 3)$-dimensional column vectors. $\boldsymbol{\Theta}$ is a $3n$-dimensional column vector, and H_k is a $(2n - 3) \times 3n$ matrix. The covariances of $\Delta z_{ij,k}$, if we assume the QUEST model for the sensor measurement errors,[12] are given by

$$E\{\Delta z_{ij,k}\} = 0 \quad , \tag{3-8}$$

$$E\{\Delta z_{ij,k} \Delta z_{ij,k}\} = (\sigma_i^2 + \sigma_j^2)(\hat{\mathbf{W}}_{i,k}^o \times \hat{\mathbf{W}}_{j,k}^o) \cdot (\hat{\mathbf{W}}_{i,k}^o \times \hat{\mathbf{W}}_{j,k}^o) \quad , \tag{3-9}$$

$$E\{\Delta z_{ij,k} \Delta z_{i\ell,k}\} = \sigma_i^2 (\hat{\mathbf{W}}_{i,k}^o \times \hat{\mathbf{W}}_{j,k}^o) \cdot (\hat{\mathbf{W}}_{i,k}^o \times \hat{\mathbf{W}}_{\ell,k}^o) \quad , \tag{3-10}$$

$$E\{\Delta z_{ij,k} \Delta z_{\ell m,k}\} = 0 \quad . \tag{3-11}$$

To demonstrate how the components of the measurement equation are formed, a simple three sensor example will be presented. The three scalar measurements are

$$z_{12,k} = \hat{\mathbf{W}}_{1,k}^o \times \hat{\mathbf{W}}_{2,k}^o \cdot (\boldsymbol{\theta}_1 - \boldsymbol{\theta}_2) + \Delta z_{12,k} \quad , \tag{3-12}$$

$$z_{13,k} = \hat{\mathbf{W}}_{1,k}^o \times \hat{\mathbf{W}}_{3,k}^o \cdot (\boldsymbol{\theta}_1 - \boldsymbol{\theta}_3) + \Delta z_{13,k} \quad , \tag{3-13}$$

$$z_{23,k} = \hat{\mathbf{W}}_{2,k}^o \times \hat{\mathbf{W}}_{3,k}^o \cdot (\boldsymbol{\theta}_2 - \boldsymbol{\theta}_3) + \Delta z_{23,k} \quad . \tag{3-14}$$

Thus, the 3×1 matrix $\mathbf{Z}_k$ is

$$\mathbf{Z}_k = [\, z_{12,k}, z_{13,k}, z_{23,k} \,]^T \quad , \tag{3-15}$$

and the 9×1 matrix $\boldsymbol{\Theta}$ is

$$\boldsymbol{\Theta} = [\, \boldsymbol{\theta}_1^T, \boldsymbol{\theta}_2^T, \boldsymbol{\theta}_3^T \,]^T = [\, \theta_{11}, \theta_{12}, \theta_{13}, \theta_{21}, \theta_{22}, \theta_{23}, \theta_{31}, \theta_{32}, \theta_{33} \,]^T \quad , \tag{3-16}$$

where the misalignment angle, θ_{ij}, in equation (3-16) refers to misalignment angle j of sensor i. The matrix H_k is formed as

$$H_k = \begin{bmatrix} (\hat{\mathbf{W}}_{1,k}^o \times \hat{\mathbf{W}}_{2,k}^o)^T & -(\hat{\mathbf{W}}_{1,k}^o \times \hat{\mathbf{W}}_{2,k}^o)^T & \mathbf{0}^T \\ (\hat{\mathbf{W}}_{1,k}^o \times \hat{\mathbf{W}}_{3,k}^o)^T & \mathbf{0}^T & -(\hat{\mathbf{W}}_{1,k}^o \times \hat{\mathbf{W}}_{3,k}^o)^T \\ \mathbf{0}^T & (\hat{\mathbf{W}}_{2,k}^o \times \hat{\mathbf{W}}_{3,k}^o)^T & -(\hat{\mathbf{W}}_{2,k}^o \times \hat{\mathbf{W}}_{3,k}^o)^T \end{bmatrix} \quad . \tag{3-17}$$

Relative alignments are defined as the alignment of an attitude sensor relative to another attitude sensor. For convenience, the sensor to which the relative alignments are being determined will be designated as sensor 1. Thus,

$$\boldsymbol{\psi}_i \equiv \boldsymbol{\theta}_i - \boldsymbol{\theta}_1 \quad , \tag{3-18}$$

28

where ψ_i is the alignment of sensor i relative to sensor 1. The $(3n-3)$-dimensional vector of relative alignments can likewise be found from the absolute alignment vector as

$$\Psi \equiv [\psi_2^T, \psi_3^T, \ldots, \psi_n^T]^T = F\Theta \quad , \tag{3-19}$$

where F is the $(3n-3) \times 3n$ matrix and is defined as

$$F \equiv \begin{bmatrix} -I_{3\times3} & I_{3\times3} & 0_{3\times3} & \ldots & 0_{3\times3} \\ -I_{3\times3} & 0_{3\times3} & I_{3\times3} & \ldots & 0_{3\times3} \\ \vdots & \vdots & \vdots & \ddots & \vdots \\ -I_{3\times3} & 0_{3\times3} & 0_{3\times3} & \ldots & I_{3\times3} \end{bmatrix} \quad . \tag{3-20}$$

From equation (3-5) it is clear that $\mathbf{Z}_k$ is sensitive only to the relative alignments and we may write

$$\mathbf{Z}_k = H_k' \Psi + \Delta \mathbf{Z}_k \quad , \tag{3-21}$$

where H_k' is the $(2n-3) \times (3n-3)$ matrix obtained by deleting the first three columns of H_k. As stated earlier, the relative alignment vector has dimension $3n-3$ and is completely observable from the inflight data.

The Attitude-Independent Inflight Estimator

Using the measurement model developed above the negative-log-likelihood function[13] may be written as

$$J_{\Psi}(\Psi) = \frac{1}{2} \sum_{k=1}^{N} \left\{ [(\mathbf{Z}_k - H_k'\Psi)^T P_{Z_k}^{-1}(\mathbf{Z}_k - H_k'\Psi)] \right.$$
$$\left. + \log \det P_{Z_k} + (2n-3)\log 2\pi \right\} \quad . \tag{3-22}$$

which is minimized to obtain the maximum likelihood estimate of the relative alignments. Minimizing this expression leads to the usual normal equations

$$P_{\Psi\Psi}^{-1}(\text{PF}) = \sum_{k=1}^{N} H_k'^T P_{Z_k}^{-1} H_k' \quad , \tag{3-23}$$

$$\Psi^*(\text{PF}) = P_{\Psi\Psi}(\text{PF}) \sum_{k=1}^{N} H_k'^T P_{Z_k}^{-1} \mathbf{Z}_k \quad , \tag{3-24}$$

where "PF" denotes *prior-free* and indicates that the estimate is based only on the inflight data and not on any prior (i.e., prelaunch) estimate of the alignments.

Determination of the Temperature Dependence of the Alignments

As was shown in section 2, the SMM yaw alignments depend on the spacecraft structural temperature variations. Thus, we seek to use maximum-likelihood estimation methods to

better quantify the dependence of the relative alignments on the temperature. The relative misalignments are assumed to depend linearly on the temperature. Thus, we write

$$\Psi_{T_i}^{\text{true}} = \mathbf{a} + \mathbf{b}\left(T_i - T_o\right) \quad , \tag{3-25}$$

where T_o is the reference temperature at which the alignments were determined during the prelaunch alignment calibration and T_i is the spacecraft structural temperature at which the inflight misalignment is estimated to yield $\Psi_{T_i}^*(\text{PF})$. We wish to compute the values of the $(3n - 3) \times 1$ coefficient vectors, $\mathbf{a}$ and $\mathbf{b}$. Thus we write,

$$\Psi_{T_i}^*(\text{PF}) = \Psi_{T_i}^{\text{true}} + \Delta\Psi_{T_i}^*(\text{PF}) \quad , \tag{3-26}$$

where

$$E\{\Delta\Psi_{T_i}^*(\text{PF})\} = \mathbf{0} \quad , \tag{3-27}$$

$$E\{\Delta\Psi_{T_i}^*(\text{PF})\Delta\Psi_{T_i}^{*T}(\text{PF})\} = P_{\Psi_{T_i}}(\text{PF}) \quad , \tag{3-28}$$

where at each temperature T_i, $\Psi_{T_i}^*(\text{PF})$ and $P_{\Psi_{T_i}}(\text{PF})$ are obtained from equations (3-23) and (3-24).

Substituting equation (3-25) into equation (3-26) yields

$$\Psi_{T_i}^*(\text{PF}) = \mathbf{a} + \mathbf{b}\left(T_i - T_o\right) + \Delta\Psi_{T_i}^*(\text{PF}) \quad , \tag{3-29}$$

and $\Psi_{T_i}^*(\text{PF})$ serves now as an effective measurement.

Defining the parameter vector

$$\Lambda = \begin{bmatrix} \mathbf{a} \\ \mathbf{b} \end{bmatrix} \quad , \tag{3-30}$$

the measurement equation becomes

$$\Psi_{T_i}^*(\text{PF}) = H_{T_i}'\Lambda + \Delta\Psi_{T_i}^*(\text{PF}) \quad , \tag{3-31}$$

where

$$H_{T_i}' = [\, I \quad I(T_i - T_o)\,] \quad . \tag{3-32}$$

The coefficient vector Λ may be obtained by minimizing the negative-log-likelihood function

$$J_\Lambda(\Lambda) = \frac{1}{2}\sum_{T_i}\left\{\left[(\Psi_{T_i}^*(\text{PF}) - H_{T_i}'\Lambda)^T P_{\Psi_{T_i}}^{-1}(\text{PF})(\Psi_{T_i}^*(\text{PF}) - H_{T_i}'\Lambda)\right] \right.$$
$$\left. + \log \det P_{\Psi_{T_i}}\right) + N_T \log 2\pi\right\} \quad , \tag{3-33}$$

where N_T is the number of temperatures at which the inflight estimates of the relative alignments has been estimated. Carrying out the minimization leads to[5]

$$P_{\Lambda\Lambda}^{-1} = \sum_{T_i} H_{T_i}'^T P_{\Psi_{T_i}}^{-1}(\text{PF}) H_{T_i}' \quad , \tag{3-34}$$

$$\Lambda^* = P_{\Lambda\Lambda} \sum_{T_i} H_{T_i}'^T P_{\Psi_{T_i}}^{-1}(\text{PF})\Psi_{T_i}^*(\text{PF}) \quad . \tag{3-35}$$

Simulations

The algorithms developed above were applied to two simulations, the first a very simple spacecraft in which the alignments do not depend on the temperature and the second a spacecraft configured like the SMM and whose alignments are temperature-dependent. For each simulation a set of model misalignments was computed in order to generate the observed and reference vectors and to judge the effectiveness of the simulated calibrations. The distribution of the misalignments was assumed to be Gaussian and zero-mean. This particular model was chosen to test an algorithm for estimating launch-shock error levels[7,9] not relevant to the SMM application as presented here.

The first simulation is of a spacecraft with three attitude sensors with well separated boresights. The model sensors were taken to have an FOV of 20 deg by 20 deg and an accuracy of 10 arc-sec. One hundred frames of simulated data were generated in which each sensor was assumed always to have valid data. The results are shown in Table 1. The agreement between the model misalignments and the estimates is consistent with the computed standard deviations.

TABLE 1

Comparison of Model and Estimated
Relative Misalignments for Simulation 1

Model Relative Misalignment (arc-sec)	Estimated Relative Misalignment (arc-sec)
−73.	−73. ± 1.
−40.	−50. ± 8.
63.	78. ± 13.
−14.	−7. ± 7.
−43.	−45. ± 1.
131.	146. ± 12.

For the second simulation, where model misalignments were needed at a range of distinct temperatures, the coefficient vector $\mathbf{b}$ was given arbitrary values while $\mathbf{a}$ was sampled from a zero-mean Gaussian distribution. The model relative misalignments at the remaining temperatures were computed from

$$\mathbf{\Psi}_{T_i} = \mathbf{a} + \mathbf{b}\,(T_i - T_o) \quad . \tag{3-36}$$

The types of sensors and their size and accuracies were modeled after the SMM FPSSs and FHSTs. The temperature range of the plate on which the FPSSs were mounted

TABLE 2
Comparison of Model and Estimated Coefficients of the
Temperature Dependence of Misalignments For Simulation 2

Model Constant Term a (arc-sec)	Estimated Constant Term a (arc-sec)	Model Linear Term b (arc-sec/°C)	Estimated Linear Term b (arc-sec/°C)
−43.	−47. ± 14.	0.	0.0 ± 5.0
0.	1. ± 1.	0.	0.2 ± 0.1
0.	−1. ± 1.	0.	0.2 ± 0.1
−44.	−52. ± 10.	60.	60.1 ± 4.0
100.	91. ± 5.	−30.	−29.9. ± 2.0
−128.	−119. ± 5.	30.	29.9. ± 2.0
158.	131. ± 11.	60.	60.1 ± 4.0
−39.	−48. ± 5.	−30.	−29.9 ± 2.0
−189.	−179. ± 5.	30.	29.9 ± 2.0

was modeled as varying between 2°C and 10°C with data generated at 2°C intervals. The reference temperature was taken as 6°C. As for the SMM, the misalignments were computed relative to the first sensor. The simulated calibration was performed at each temperature and the results were collected and used in the algorithm of equations (3-34) and (3-35) to estimate the dependence of the misalignments on temperature.

The results are shown in Table 2. Again the agreement between the model and estimated alignments is consistent with the computed standard deviations. Thus, for both simulations the algorithms worked well and provided meaningful error bounds.

4. APPLICATION TO THE SMM

In this section the newly derived algorithms will be applied to data from the SMM in order to better quantify the dependence of the SMM alignments on temperature variations. In addition, the limiting assumptions made during the SMM prelaunch analysis will also be examined in greater detail.

Application of Algorithms to SMM Data

Since this study was conducted nearly five years after the data from the heuristic analysis was collected, provisions had to be made to collect sufficient statistics. In order to make the best comparisons, it was decided to examine the data from after the repair of the SMM

until the time of the first null redefinition in December of 1984. During this time, the SMM structural temperatures ranged from 12.12°C to 20.16°C. It was attempted to collect three orbits of data at each discrete temperature point. However, to obtain good observability of the alignments, data must be well spread throughout a sensor field-of-view. Since the spacecraft was pointed so that the Sun would be very close to the FPSS boresight, it was difficult to obtain much variation in the FPSS observations, even by combining all data sets at the same temperature. Thus, it was impossible to gain any observability about the roll axes of the FPSSs (which in turn prevented any observability of the roll axes of the FHSTs relative to the FPSSs).

Despite this limitation of the data, the calibrations were carried out and the results are shown in Fig. 3 through Fig. 6. These graphs show several very interesting results. First, as unseen from the heuristic analysis, a temperature dependence about the pitch axis is evident. The slope of the dependence seems to be nearly the same as that of the yaw dependence but opposite in sign. Thus, it remained to determine why this was occurring. It is possible that noise from other effects obscured the pitch dependence during the heuristic analysis.

The main source of noise in the pseudo-alignment solutions was from the FHST attitude solutions. The accuracy of these solutions depended on the quality of the star fields observed by the FHSTs. Thus, in order to resolve the discrepancy between the two results, the pitch data from the heuristic analysis was reduced. The first step was to identify periods of time when poor star fields were used by the pseudo-alignment algorithm. It turned out that periods could be found, of length one to two weeks, where poor star data was used that greatly increased the noise level in the solutions. Elimination of these periods and replotting of the remaining data as a scatter plot of temperature and pitch misalignment results in a nearly linear dependence with slope opposite that of the yaw misalignment. This plot is shown in Fig. 7. Thus, after this further analysis, it appears the two methods agree.

The second point to notice from Figs. 3 through 6 is that the slopes of the dependence using the new algorithms are opposite those gained from the heuristic analysis. This can be seen to be correct when it is recalled that the pseudo-alignments were calculated by subtracting the FHST attitude solution from the FPSS attitude solution. Thus, the pseudo-alignments were actually, according to equation (3-18), alignments of the FPSSs relative to the FHSTs. Since this is opposite to what was computed by the new algorithms, it would be expected that the earlier slopes would be opposite in sign.

Using the algorithms developed above to compute the actual temperature dependence of the alignments, the coefficients were solved for and the results are shown in Table 3. As can be seen, the linear dependence was significant about both the pitch and yaw axes. The magnitude of the dependence as calculated by the new algorithms was several times greater than that computed by the heuristic methods because the latter was masked by the larger random errors in the alignments.
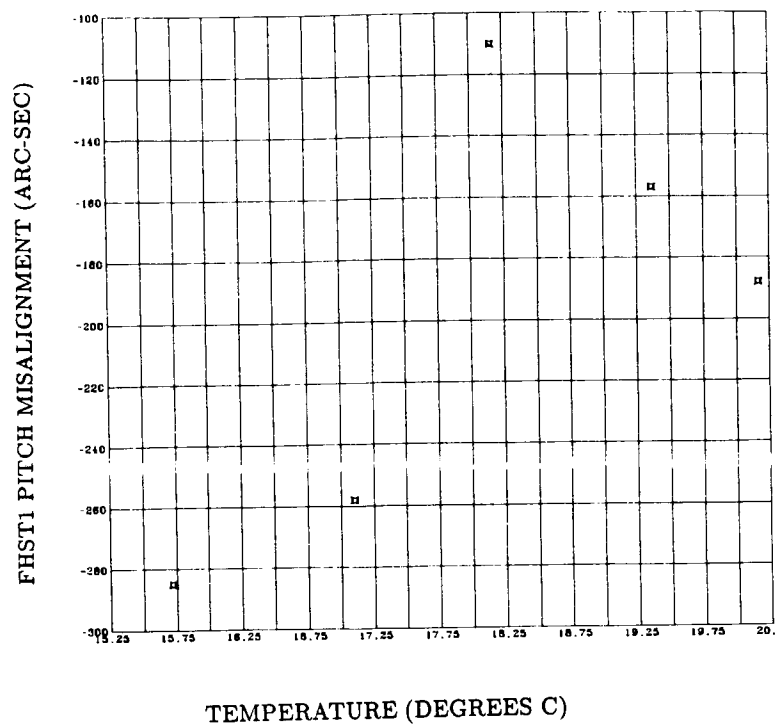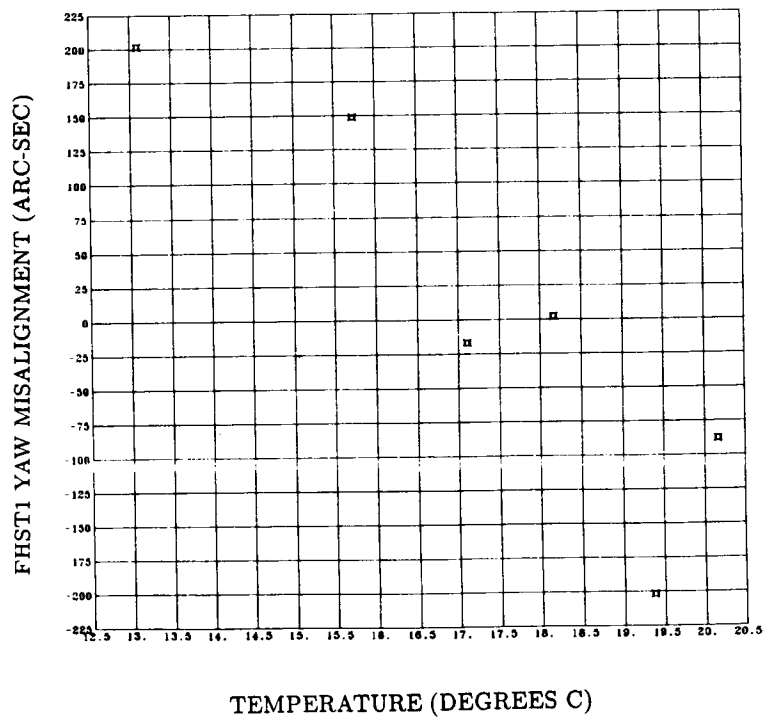
Figure 3. FHST1 Pitch Misalignment
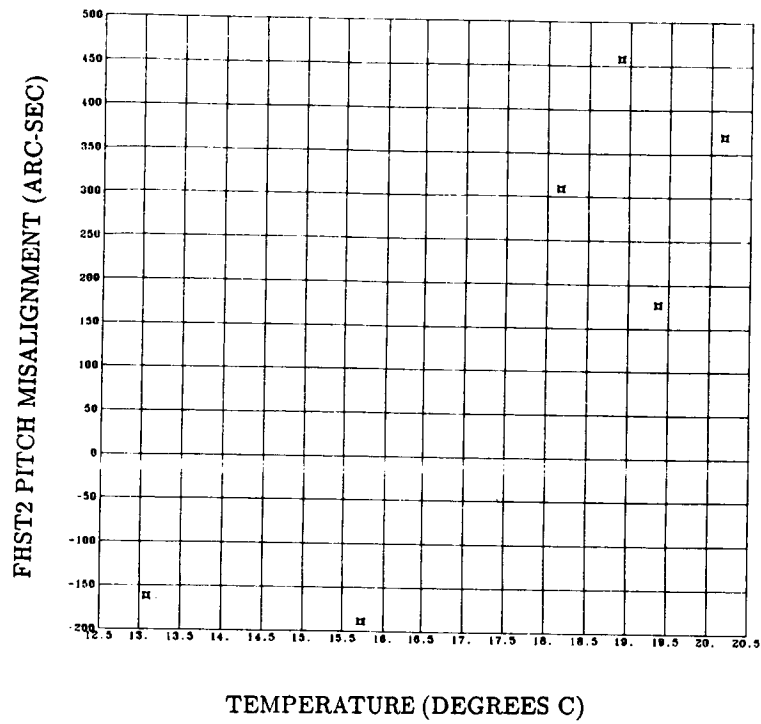

Figure 4. FHST1 Yaw Misalignment

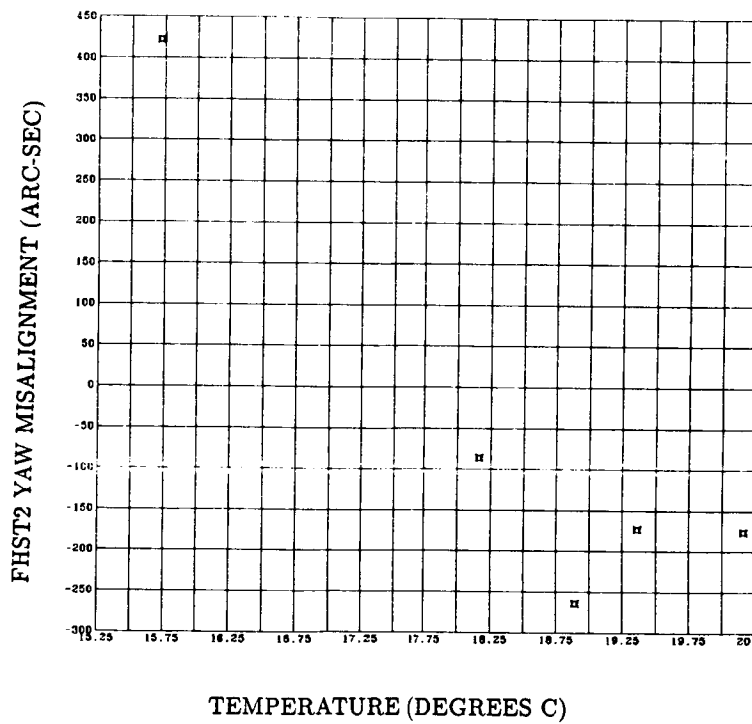34

Figure 5. FHST2 Pitch Misalignment

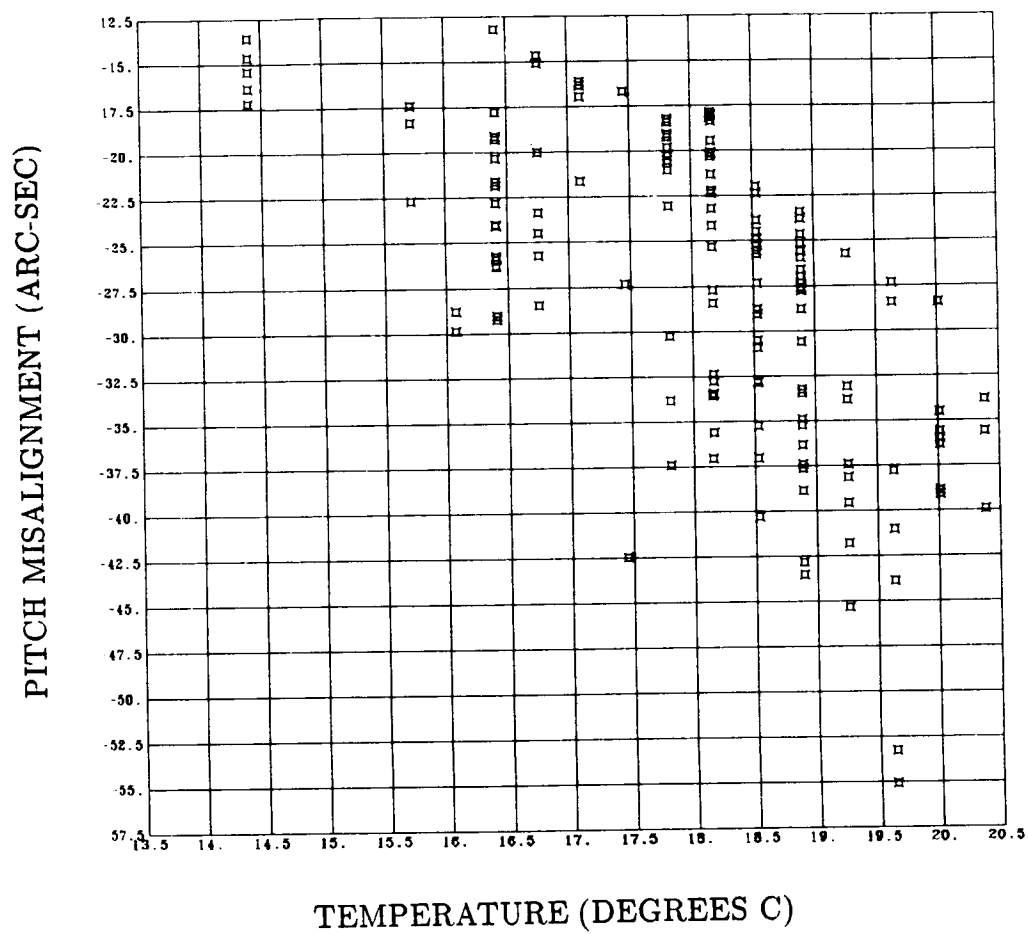
Figure 6. FHST2 Yaw Misalignment

Figure 7. Reduced Pitch Misalignment Data

TABLE 3

Coefficients of the Temperature Dependence of the Alignments
Relative to Solar Maximum Mission Fine Pointing Sun Sensor 1

Sensor Axis	Constant Term a (arc-sec)	Linear Term b (arc-sec/°C)
FPSS2 PITCH	0.7 ± 0.1	0.0 ± 0.0
FPSS2 YAW	0.5 ± 0.1	0.0 ± 0.0
FHST1 PITCH	-164.7 ± 3.7	37.1 ± 1.4
FHST1 YAW	17.8 ± 4.3	-33.5 ± 1.7
FHST2 PITCH	278.2 ± 2.9	48.0 ± 1.1
FHST2 YAW	-100.8 ± 3.4	-40.9 ± 1.3

Thus, there is good agreement between the two methods about the nature and dependence of the SMM FHST pitch and yaw alignments relative to the FPSSs. The new algorithms clearly show better results because they avoid the large error sources that caused the heuristic methods to miss the pitch alignment dependence and they treated the alignments of the FHSTs separately which provided better information as to the actual behavior of each one.

Examination of SMM Alignment Assumptions

As stated earlier, two assumptions were made regarding the expected nature of the SMM fine attitude sensor alignments. In this section, each assumption will be examined to ascertain its validity.

The first assumption was that the alignment of the SMM payload relative to the FPSSs would not change from its prelaunch value of zero. While no real data is available from the SMM scientific instruments to be used in any alignment algorithm, this assumption could still be tested. Since there were two FPSSs that were mounted on the instrument support plate along with the scientific payload, any alignment variation between the FPSSs should be of the same order of magnitude as that between the FPSSs and the payload. Thus, the alignment of the FPSSs relative to each other was studied using the new algorithms. This study showed that the alignment of FPSS2 relative to FPSS1 showed no significant variation, and the values of the misalignment angles were never greater than 1 or 2 arc-sec. Thus, the assumption that the payload alignment never varied can be judged as valid from the limited information available.

The second assumption was that no roll alignment information involving the FPSSs was observable. As stated in Ref. 6, all the relative alignments are observable, and since the alignments of the SMM were computed relative to FPSS1, they should all be observable. However, the observability of the alignment about an axis depended on the spread of data

in the sensors that are sensitive to that axis. Because all the data that was examined in the previous section had a poor spread in the FPSS, poor observability was obtained about the FPSS roll axis. In fact, this is the crux of the assumption that no observability is possible about this axis because the spread could never be good. However, it is asserted here that if a good spread could be obtained, the SMM roll axis misalignment could have been determined within a reasonable error. Thus, data with a good spread in the FPSS FOV had to be found.

It was discovered that data from the SMM that had a good spread in the FPSS FOV was available. During the times of the FPSS electronic response calibrations, that calibrated the transformation of FPSS measurements in units of FPSS counts to degrees, the SMM was rotated in such a way that the observed Sun vector had a significant variation in the FPSS FOV. This data was obtained and the calibration was performed. The computed alignments had variances of 60 arc-sec for the determination of the FHST roll alignments. During the normal calibrations when the spread of data was poor, the variance was close to ten thousand arc-sec. Thus, the simple rotations during the electronic response calibrations provided great improvement in the misalignment determination capability.

During the electronic response calibrations, the rotations were as large as one quarter of a degree; thus, the angle between the spacecraft to Sun vector and the FPSS boresight vector reached one quarter of a degree. Since the FPSS field-of-view was 2 deg by 2 deg, this Sunline angle could have conceivably reached one degree. However, no usable data was available where the Sunline angle was greater than one quarter of a degree. Thus, as a test of the possible observability of the SMM roll misalignments, simulations were done, using the exact SMM configuration, that increased the Sunline angle to one half degree and one degree to improve the spread of data in the FPSS field-of-view. The misalignment calibrations at one half degree decreased the variance of the roll misalignment solutions to 30 arc-sec and the misalignment calibrations at one degree lowered the variance to 16 arc-sec. Thus, by simply rotating the spacecraft to the full capability of the SMM FPSSs, full observability of all the misalignments could have been obtained.

5. CONCLUSIONS

A full analysis of the nature of the fine attitude sensor alignment behavior on the Solar Maximum Mission has been presented. The dependence of the alignments on the spacecraft structural temperature variations has been investigated, and results have shown that simple equations could be derived to fully account for the dependence. In addition, an assumption on the observability of the alignments has been shown to be unnecessary. The results of this work can be applied by other missions so that they may be able to explain the variations in the sensor alignments.

6. REFERENCES

[1] Hewitt, D., *Multimission Modular Spacecraft (MMS) Thermal System Specification*, Goddard Space Flight Center, S-700-12, February 1977.

[2] Patt, F., *Analysis of the Solar Maximum Mission (SMM) Fine Pointing Sun Sensor (FPSS) Response Changes*, Computer Sciences Corporation, CSC/TM-85/6714, May 1985.

[3] Pitone, D., Eudell, A., and Patt, F., "Temperature Dependence of Attitude Sensor Coalignments on the Solar Maximum Mission," *Proceedings, Flight Mechanics/Estimation Theory Symposium*, NASA Goddard Space Flight Center, Greenbelt, Maryland, May 1989.

[4] Pitone, D., Eudell, A., and Patt, F., "Temperature Dependence of Attitude Sensor Coalignments on the Solar Maximum Mission," *Proceedings, AIAA/AAS Astrodynamics Specialist Conference*, Stowe, Vt., August 1989.

[5] Pitone, D., *The Estimation of Attitude Sensor Misalignment Due to Spacecraft Bending on the Solar Maximum Mission*, Masters Thesis, Howard University, May 1990.

[6] Pitone, D., *Solar Maximum Mission End-of-Mission Document*, Computer Sciences Corporation, CSC/TM-90/6058, April 1990.

[7] Shuster, M. D., Pitone, D. S., and Bierman, G. J., "Batch Estimation of Spacecraft Sensor Alignments, "submitted to *the Journal of the Astronautical Sciences*.

[8] Bierman, G. J., and Shuster, M. D., "Spacecraft Alignment Estimation," *Proceeedings, 27th IEEE Conference on Decision and Control*, Austin, Texas, December 1988.

[9] Shuster, M. D., and Pitone, D. S., "Consistent Estimation of Spacecraft Sensor Alignments," *Proceedings, American Control Conference*, San Diego, California, May 1990.

[10] Shuster, M. D., "Inflight Estimation of Spacecraft Sensor Alignment," *Proceedings, 13th AAS Guidance and Control Conference*, Keystone, Colorado, February, 1990.

[11] Wertz, J., (Ed.), *Spacecraft Attitude Determination and Control*, D. Reidel, Dordrecht, the Netherlands, 1978.

[12] Shuster, M. D. and Oh, S. D., "Three-Axis Attitude Determination from Vector Observations," *Journal of Guidance and Control*, Vol. 4, pp. 70–77, 1981.

[13] Sorenson, Harold, *Parameter Estimation*, Marcel Dekker, New York and Basel, 1980.